A Noninvasive Method for Assessing Impaired Diastolic Suction in Patients With Dilated Cardiomyopathy

Raquel Yotti, Javier Bermejo, J. Carlos Antoranz, M. Mar Desco, Cristina Cortina, José Luis Rojo-Álvarez, Carmen Allué, Laura Martín, Mar Moreno, José A. Serrano, Roberto Muñoz and Miguel A. García-Fernández

Circulation 2005;112;2921-2929
DOI: 10.1161/CIRCULATIONAHA.105.561340
Circulation is published by the American Heart Association. 7272 Greenville Avenue, Dallas, TX 72514
 Print ISSN: 0009-7322. Online ISSN: 1524-4539

A Noninvasive Method for Assessing Impaired Diastolic Suction in Patients With Dilated Cardiomyopathy

Raquel Yotti, MD; Javier Bermejo, MD, PhD; J. Carlos Antoranz, PhD; M. Mar Desco, MD, PhD; Cristina Cortina, MD; José Luis Rojo-Álvarez, MEng, PhD; Carmen Allué, RDNS; Laura Martín, BSc; Mar Moreno, MD; José A. Serrano, MD; Roberto Muñoz, MD, PhD; Miguel A. García-Fernández, MD, PhD

Background—Diastolic suction is a major determinant of early left ventricular filling in animal experiments. However, suction remains incompletely characterized in the clinical setting.

Methods and Results—First, we validated a method for measuring the spatio-temporal distributions of diastolic intraventricular pressure gradients and differences (DIVPDs) by digital processing color Doppler M-mode recordings. In 4 pigs, the error of peak DIVPD was 0.0±0.2 mm Hg (intraclass correlation coefficient, 0.95) compared with micromanometry. Forty patients with dilated cardiomyopathy (DCM) and 20 healthy volunteers were studied at baseline and during dobutamine infusion. A positive DIVPD (toward the apex) originated during isovolumic relaxation, reaching its peak shortly after mitral valve opening. Peak DIVPD was less than half in patients with DCM than in control subjects (1.2±0.6 versus 2.5±0.8 mm Hg, $P<0.001$). Dobutamine increased DIVPD in control subjects by 44% ($P<0.001$) but only by 23% in patients with DCM (P=NS). DIVPDs were the consequence of 2 opposite forces: a driving force caused by local acceleration, and a reversed (opposed to filling) convective force that lowered the total DIVPD by more than one third. In turn, local acceleration correlated with E-wave velocity and ejection fraction, whereas convective deceleration correlated with E-wave velocity and ventriculo:annular disproportion. Convective deceleration was highest among patients showing a restrictive filling pattern.

Conclusions—Patients with DCM show an abnormally low diastolic suction and a blunted capacity to recruit suction with stress. By raising the ventriculo:annular disproportion, chamber remodeling proportionally increases convective deceleration and adversely affects left ventricular filling. These previously unreported mechanisms of diastolic dysfunction can be studied by using Doppler echocardiography. **(*Circulation*. 2005;112:2921-2929.)**

Key Words: cardiomyopathy ■ echocardiography ■ heart failure ■ imaging ■ diastole

Diastolic function heavily influences the symptomatic status and outcome of patients with dilated cardiomyopathy (DCM).[1,2] In the clinical setting, left ventricular (LV) diastolic function is characterized in terms of relaxation, compliance, and filling pressures, usually assessed indirectly by Doppler echocardiography. However, a number of additional physiological factors influence diastolic function.[3] Among them, diastolic suction has shown to actively contribute to rapid filling, and is a mechanism by which the LV can accept an adequate filling volume at low pressure.[4,5] Thus, diastolic suction is a major determinant of LV filling dynamics.

Editorial p 2888

Three definitions of diastolic suction have been proposed.[6] First, the term diastolic suction was coined to describe the phenomenon of the left ventricle decreasing its pressure despite its filling during early diastole.[7] Second, by inducing nonfilling beats, the term diastolic suction has been used to account for the capacity of the LV to generate a subatmospheric pressure during early diastole.[5,8,9] Finally, diastolic suction has been also defined as the physiological diastolic intraventricular pressure gradient (DIVPG) generated between the apex and the base during early diastole.[10–14] Although these 3 definitions are not the same in strict physical terms, they are very closely related,[13] follow similar physiological determinants, and cause analogous effects on filling.[12,14–18] Thus, we hypothesized that the analysis of DIVPGs could allow investigators to extrapolate these basic concepts of diastolic suction to the clinical setting.

Well-established fluid dynamic principles explain the mechanisms by which DIVPGs are generated. Regional

Received May 10, 2005; revision received June 28, 2005; accepted July 15, 2005.

From the Department of Cardiology (R.Y., J.B., C.C., C.A., M.M., J.A.S., R.M., M.A.G.-F.) and the Unit of Experimental Medicine and Surgery (M.M.D.), Hospital General Universitario Gregorio Marañón, Madrid, Spain; the Department of Mathematical Physics and Fluids (J.C.A., L.M.), Facultad de Ciencias, Universidad Nacional de Educación a Distancia, Madrid, Spain; and the Department of Signal Theory and Communications (J.L.R.-A.), Universidad Carlos III de Madrid, Spain.

Correspondence to Dr Javier Bermejo, Department of Cardiology, Hospital General Universitario Gregorio Marañón Dr Esquerdo 46, 28007 Madrid, Spain. E-mail javbermejo@jet.es

Circulation **is available at http://www.circulationaha.org** **DOI: 10.1161/CIRCULATIONAHA.105.561340**

pressure gradients result from the interaction of inertial (local) and convective forces caused by unsteady intracardiac flows. In turn, inertial and convective forces obey different physiological determinants. Theoretically, the inertial component of DIVPG should be caused by the impulse developed by myocardial restoring forces related to the inotropic state.[8,16] The convective DIVPG should be determined by filling flow velocity and chamber geometry.[19]

According to these principles, an abnormal generation of diastolic suction is expected in patients with DCM because remarkable changes of chamber geometry coexist with uncoordinated wall motion and impaired myocardial contractility. However, the bases of diastolic suction remain almost unexplored in humans because of the need of sophisticated catheterization procedures.

In the last few years, a new noninvasive method has been proposed to measure regional pressure differences within the heart.[20–24] On the basis of digital processing of color Doppler M-mode (CDMM) images, the method has been validated to measure the diastolic intraventricular pressure difference (DIVPD) between the LV apex and the base.[21,22] We have shown that the method can be extended to visualize the spatio-temporal distribution of DIVPGs as well as to quantify separately their inertial convective components.[20] The aim of the present study is to characterize LV diastolic suction as a potential mechanism of impaired diastolic function in patients with DCM using this method. Additional objectives are to analyze, for the first time in humans, the physiological basis of DIVPGs as well as their spatial and temporal distribution. The impact of the inotropic state on DIVPGs is assessed by low-dose dobutamine infusion. The color M-mode analysis method is validated experimentally in animals before performing the clinical studies, and a group of young healthy volunteers is studied for comparison.

Methods

Patient Population

Forty patients diagnosed of DCM were prospectively enrolled on the basis of the following inclusion criteria: (1) ejection fraction (EF) <30%, (2) LV volumes >2 SD normal values for age and gender, and (3) sinus rhythm with 2 identifiable waves in the transmitral Doppler spectrogram. A subgroup of 20 subjects who were not receiving β-blocker therapy and had no history of sustained ventricular tachycardia was selected for dobutamine stimulation. Also, 20 healthy volunteers were studied as reference. Volunteers were not taking any medication, and cardiovascular disease was ruled out by history, clinical examination, ECG, and Doppler echocardiography. The study protocol was approved by the institutional ethical committee, and written informed consent was obtained from all subjects. The effects of dobutamine on ejection hemodynamics in these populations has been previously reported.[23]

Echocardiographic Image Acquisition and Analysis

A 2.0- to 3.5-MHz broadband ultrasound transducer was used on a Sequoia C-256 system (Siemens AG). End-diastolic and end-systolic diameters and volumes, as well as end-systolic wall stress (σ), were calculated from standard M-mode and biplane 2-dimensional images. As additional indexes of LV systolic chamber function, rate-corrected velocity of circumferential fiber shortening (V_{cf}) and the peak ejection intraventricular pressure difference between the apex and outflow tract (EIVPD)[23,24] were obtained from short-axis 2-dimensional and CDMM recordings, respectively. The mitral annulus diameter was measured in the 4-chamber (d_1) and 2-chamber (d_2) apical views, and its cross-sectional area was calculated as $\pi \cdot d_1 \cdot d_2/4$. Ventriculo:annular disproportion was obtained as the ratio between the cross-sectional areas of the LV base at end-systole and of the mitral annulus. The isovolumic relaxation time, peak mitral flow velocities of the early (E) and late (A) filling waves, and the E-wave acceleration and deceleration times were measured with the use of pulsed-wave Doppler. In patients with DCM, the LV filling pattern was defined as restrictive either if the E/A ratio was ≥2 or if it was between 1 and 2 and the E-wave deceleration time was ≤140 ms.[25]

CDMM images were obtained from a transthoracic 4-chamber apical view at baseline and during dobutamine infusion (10 μg/kg per minute). The method and processing algorithms used to measure pressure gradient maps has been previously reported[20] and validated for the measurement of the ejection pressure difference between the apex and the outflow tract.[23,24] A similar approach to measure total DIVPDs between the apex and the mitral annulus has been previously validated by other investigators in experimental[21] and clinical settings.[22] Briefly, if the M-mode cursor closely approximates a flow streamline, the spatio-temporal velocity distribution of a discrete blood sample ($v[s,t]$, where v represents velocity, s represents position, and t is time) is obtained by the value of its corresponding pixel color. Thus, the CDMM recording provides the data necessary to solve Euler's momentum equation:

$$\frac{\partial p}{\partial s} = -\rho \cdot \left(\underbrace{\frac{\partial v}{\partial t}}_{Inertial} + \underbrace{v \cdot \frac{\partial v}{\partial s}}_{Convective} \right)$$

where p designates pressure and ρ is blood density. As shown in the expression, the inertial and convective components of DIVPGs can be measured separately by solving the first and second term in the right side of the equation independently. DIVPG fields are displayed as color overlays representing the pressure difference (in mm Hg/cm) between one pixel and another one located 1 cm closer to the ultrasound transducer.[20,23,24] For the present study, DIVPD curves between the apex and the mitral annulus were generated by spatial integration between these 2 positions. Instead of using fixed distances between stations, the position of the apex and the mitral annulus were manually traced in each DIVPG image, based on the color and gray scale layers. The time to onset, the peak, and the time-to-peak were measured from the DIVPD curves. The peak and time-to-peak of the inertial and convective components of the DIVPD curves were also obtained. Onset and end of transmitral LV filling were determined visually from the raw CDMM image. In all figures and charts, the temporal reference was established at the time of QRS onset. However, all temporal measurements of DIVPD and flow-velocity curves are referred to the onset of filling; negative values therefore account for features that take place before mitral valve opening. The onset of DIVPD was defined as the first instant when DIVPD was >0. Flow propagation velocity was calculated semiautomatically by identifying the 50% isovelocity line from the CDMM image (Figure 1).[26] To quantify the delay observed in the longitudinal propagation of the DIVPG field from the mitral annulus to the apex, a specific index was derived. A gradient time delay (expressed in milliseconds) was measured from the DIVPG image, as the time it takes the peak early-diastolic DIVPG to propagate from the mitral annulus to a fixed apical position (3.7 cm apart). This criterion replicates a method used for measuring flow propagation time delay.[27] All pulsed-wave, M-mode, CDMM, DIVPG, and DIVPD measurements were obtained by averaging 3 consecutive beats.

Experimental Validation of DIVPG Parametrical Images

Before performing clinical studies, we validated the method against high-fidelity micromanometers. For this purpose, 4 minipigs (weight, 54±13 kg; Insituto Madrileño de Investigación y Desarrollo Rural, Agrario y Alimentario [IMIDRA], Madrid, Spain) were studied in an open-chest, closed-pericardium, instrumentation model, following a previously described protocol.[23] The animal study was approved by the local institutional animal care committee and conformed to Guiding Principles in Care and Use of Animals. A

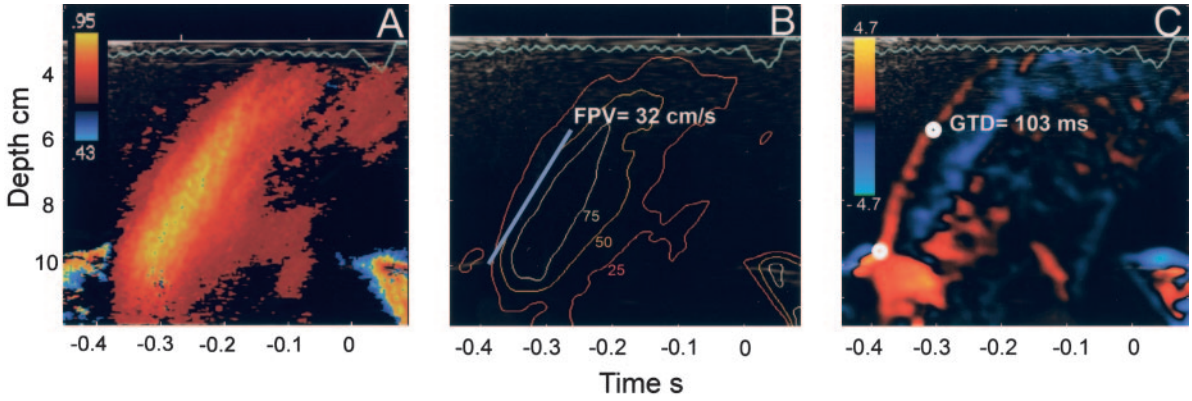

Figure 1. Methods used for measuring flow propagation velocity and gradient time delay. A, Raw flow velocity color Doppler M-mode recording. B, Isovelocity lines generated automatically representing the 25% (red), 50% (orange), and 75% (white) velocity values of the peak E-wave velocity. The leftmost front of the 50% isovelocity contour is fitted by orthogonal linear regression. Flow propagation velocity (FPV) is calculated as the slope of this line. C, DIVPG image, in which the gradient time delay (GTD) is estimated as the time between peak DIVPG values obtained at the mitral annulus and another point located 3.7 cm closer to the apex.

needle micromanometer (Millar Instruments) was inserted from the epicardium inside the LV apex. A dual-micromanometer catheter (3-cm sensor spacing, Millar Instruments) was placed through a pulmonary vein into the left atrium and then advanced to place the proximal sensor at the LV base and the distal sensor at the midcavity. Pressure transducers were balanced and calibrated in vivo.[23] Simultaneous CDMM recordings and high-fidelity pressure signals were acquired at baseline, during cava, and during aortic occlusion, under several hemodynamic states induced by β-adrenergic drug interventions.[23] Three consecutive beats were recorded during end-expiration apnea from each state-load condition. Invasive DIVPD curves between mitral annulus–apex, mitral annulus–mid LV, and mid LV–apex were calculated off-line by subtraction of the respective simultaneous pressure tracings. Doppler DIVPD curves were obtained from the DIVPG maps by spatial integration between catheter-matched locations. These positions were identified by using the gray scale image layer and 2-dimensional echocardiographic sequences recorded at the beginning of each acquisition.[23] Invasive and Doppler DIVPD curve parameters were measured blinded to the other technique.

In 342 beats analyzed, a very close agreement was observed between Doppler and invasive measurements of DIVPD curve parameters for the 3 pairs of ventricular stations (Table 1 and Figure 2). Onset of DIVPD took place earlier between the base and mid-LV cavity than between mid-LV and apex at all hemodynamic states. Doppler and invasive measurements of this temporal offset were also very close (absolute error $=6\pm15$ ms, intraclass correlation coefficient [R_{ic}]$=0.7$, $P<0.001$).

Variable Selection and Statistical Analysis

Quantitative variables are expressed as mean±SD. Paired and unpaired Student's t tests and Wilcoxon tests were used where appropriate. For the analysis of physiological determinants of the DIVPD and its components, baseline data from volunteers and patients were pooled. Notice that the physiological determinants of DIVPDs can be inferred from Euler's equation. Hence, the analysis of DIVPD determinants was designed to assess the role of physiological variables, selected a priori on the basis of this expression. Local flow acceleration is caused by the elastic recoil that follows systolic contraction and was approximated by EF as well as by V_{cf} and EIVPD. Spatial flow deceleration is caused by geometrical expansion and was approximated by the ventriculo:annular disproportion. Importantly, according to Euler's equation, the association of these variables with DIVPDs needs to be analyzed using a multivariate design. Saturated models including these 3 variables and their interactions were entered, and the final models were selected by fast backwards elimination on factors (S-Plus v. 6.1, and Design and Hmisc libraries).[28] The potential value of additional variables (heart rate, end-systolic volume, and isovolumic relaxation time) was ruled out by the same method. Standardized regression (β_{stand}) and partial correlation coefficients were calculated for the final models. A probability value of <0.05 was considered significant.

Results

Baseline DIVPGs in Volunteers and Patients

Clinical and Doppler data are summarized in Table 2 and Table 3. DIVPDs onset took place during the isovolumic relaxation period. Although their total filling time was shorter, DIVPD onset started later in patients with DCM than in volunteers (Table 3). Also, the peak DIVPD was reached later in patients, and total peak DIVPD was lower than in volunteers. Analysis of DIVPG maps demonstrated that DIVPGs originated near the base and then propagated toward the apex (Figure 3 and Figure 4). This propagation was

TABLE 1. Animal Validation of Diastolic Intraventricular Pressure Gradient Parametric Images

	Absolute Error, mm Hg or ms	Relative Error, %	R_{ic}
Peak DIVPD, mm Hg			
All locations	0.0±0.2	1±25	0.96
Base–midcavity	−0.1±0.2	−2±22	0.94
Midcavity–apex	0.1±0.2	11±45	0.96
Base–apex	0.0±0.2	−1±18	0.95
Time to DIVPD onset, ms			
All locations	−4±11	2±6	0.97
Base–midcavity	−7±9	3±5	0.97
Midcavity–apex	−1±12	1±7	0.96
Base–apex	−4±11	2±5	0.97
Time to peak DIVPD, ms			
All locations	−11±14	7±10	0.94
Base–midcavity	−16±14	10±10	0.92
Midcavity–apex	−9±9	7±9	0.97
Base–apex	−8±14	6±10	0.95

R_{ic} indicates intraclass correlation coefficient.

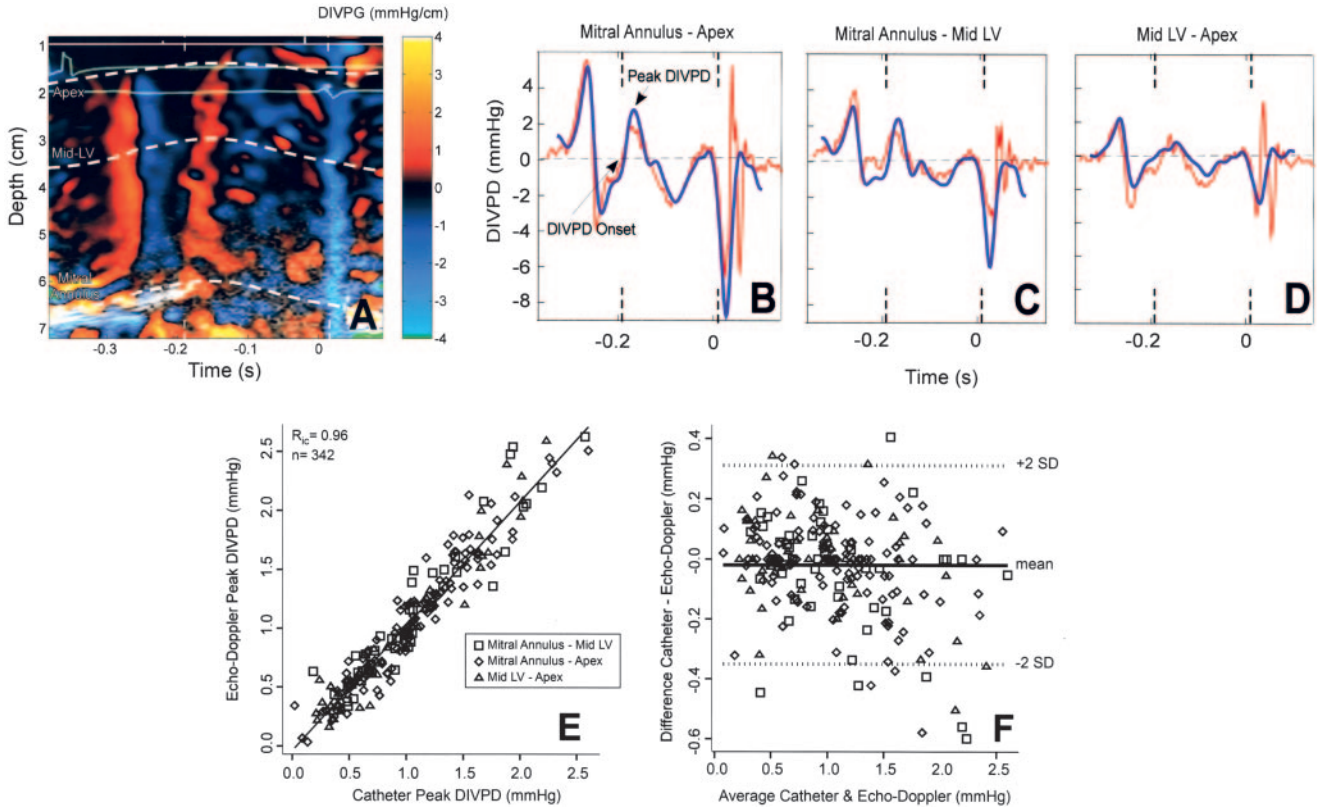

Figure 2. Experimental validation study. A, DIVPG image from a representative example. Micromanometer positions at the LV apex, mid-LV cavity, and mitral annulus are overlaid as white dotted lines. B through D, DIVPD curves obtained by echo Doppler (blue) and micromanometers (red) for positions shown in A. E through F, Linear correlation and Bland-Altman analyses of the agreement between techniques.

slower in patients with DCM because their gradient time delay was significantly prolonged (Table 3 and Figure 3).

Inertial and Convective DVIPDs: Mechanisms of Reduced DIVPDs in DCM

Analysis of DIVPD components demonstrated that the positive apex-to-base pressure drop was caused by the inertial acceleration of blood (Table 3 and Figure 3G and 3H). This positive DIVPD therefore generated a favorable suction force (pressure drop from base to apex) to accommodate the filling volume. In contrast, convective forces decelerated blood flow and generated a negative gradient (pressure rise from base to apex) in opposition to flow. Because the total DIVPD is the resultant of the instantaneous sum of these two pressure gradients of opposite sign, the total DIVPD was smaller than the inertial DIVPG component (Table 3). The peaks of the inertial and convective DIVPD components were not reached simultaneously. Nevertheless, the peak total DIVPD closely correlated with the peak value of these 2 components: Total DIVPD=0.2+0.88 · Inertial DIVPD+0.40 · Convective DIVPD (adjusted R^2= 0.85, $P<0.0001$). Space-domain analysis showed that the negative convective DIVPG was generated close to the cardiac base (Figure 4).

Patients with a restrictive filling pattern (n=15, 38%) showed similar values of total DIVPD, a trend toward a higher inertial DIVPD, and a significantly higher absolute convective DIVPD than patients with nonrestrictive filling (Figure 5). There was no difference in total, inertial, or convective DIVPDs between patients with ischemic and nonischemic DCM (1.2±0.6 versus 1.2±0.6, 2.1±1.1 versus 1.9±1.0, and −1.9±1.3 versus −1.7±1.2 mm Hg, respectively, $P>0.4$ for all).

Effects of β-Adrenergic Stimulation

Dobutamine data from 2 patients with DCM were unavailable because of fusion of the E and A waves. Inotropic stimulation significantly increased DIVPDs in volunteers but not in patients with DCM (Table 3). Split analysis of patients with ischemic and nonischemic DCM showed an absence of significant response to dobutamine in either group ($P=0.6$ and $P=0.4$, respectively).

Physiological Correlates of DIVPDs

The peak inertial DIVPD was related to E-wave velocity and EF (Table 4). The peak convective DIVPD was related to E-wave velocity, the ventriculo:annular disproportion, and their interaction. The total DIVPD was related to EF, the ventriculo:annular disproportion, and its interaction with E-wave velocity. The isolated effect of E-wave velocity was removed in the final model of total DIVPD because its opposite effects on the inertial and convective components canceled out (Table 4). Identical models were obtained when V_{cf} or EIVPD was entered in place of EF for predicting inertial (V_{cf} $\beta_{stand}=0.51$, $P<0.001$, adjusted $R^2=0.66$; EIVPD

TABLE 2. Clinical Data

	Patients With Dilated Cardiomyopathy			Healthy Volunteers (n=20)	
	Full Group (n=40)	Stress Group (n=20)			
		Baseline	Dobutamine	Baseline	Dobutamine
Age, y	61±13†	62±11		29±3	
Gender (male/female)	24/16	14/6		10/10	
NYHA functional class, n (%)					
I	9 (22)	3 (15)		...	
II	18 (45)	6 (30)		...	
III	13 (32)	11 (55)		...	
Weight, kg	72±15	69±15		69±12	
Ischemic cardiomyopathy, n (%)	18 (45)†	11 (55)		...	
QRS>120 ms, n (%)	15 (38)†	10 (50)		0 (0)	
Mitral annulus area, cm^2	6.8±0.8†	7.0±0.9		6.2±0.7	
Heart rate, beats/min	74±13	77±8	90±15*†	72±7	92±14*†
Systolic blood pressure, mm Hg	116±20	107±19	125±33*†	117±12	139±17*†
Diastolic blood pressure, mm Hg	68±12	64±14	64±14	59±9	59±7
Rate-corrected V_{cf}, s^{-1}	0.9±0.3†	0.9±0.4	1.2±0.6*†	2.0±0.2	2.7±0.3*†
EIVPD, mm Hg	3.1±1.0†	3.5±1.0	5.5±2.0*†	4.7±1.3	9.5±2.2*†
σ, g/cm^2	144±47†	140±44	136±62†	57±14	49±19*†
LV end-diastolic volume, mL	181±61†	177±47	174±58†	91±16	76±14*†
LV end-systolic volume, mL	139±56†	133±38	116±48†	32±7	19±5*†
LV ejection fraction, %	24±8†	25±7	35±9*†	65±5	76±5*†

V_{cf} indicates rate-corrected velocity of circumferential fiber shortening of the LV; EIVPD, ejection apex-to-LVOT intraventricular pressure difference; σ, LV end-systolic meridional wall stress.

*$P<0.05$, dobutamine vs baseline; †$P<0.05$, patients with dilated cardiomyopathy vs healthy volunteers for the same phase.

$\beta_{stand}=0.32$, $P<0.001$, adjusted $R^2=0.50$) and total DIVPDs (Vcf $\beta_{stand}=0.44$, $P=0.002$, adjusted $R^2=0.57$; EIVPD $\beta_{stand}=0.25$, $P=0.02$, adjusted $R^2=0.54$).

Discussion

The present study demonstrates a previously unreported mechanism of impaired filling in patients with DCM. Using a fully noninvasive method, we evidenced that cardiomyopathic ventricles have a reduced capacity to generate suction as well as a blunted suction response to stress. This mechanism may contribute to the abnormally elevated filling pressures typically found in these patients. In terms of flow dynamics, reduced suction resulted from lower inertial flow acceleration and proportionally higher deleterious convective deceleration. In terms of physiological variables, reduced suction resulted from reduced global elastic recoil and abnormal chamber geometry. Although a number of these findings have been reported in animals, they had never been demonstrated in humans.

Diastolic Suction, DIVPGs, and LV Filling

Established experimental evidence supports the idea that the LV actively "sucks" blood from the left atrium during early diastole. Importantly, in terms of flow-driving energy expenditure, diastolic suction contributes to filling more than one order of magnitude above passive atrial decompression.[29] Our temporal analysis confirms in humans that suction is initiated during isovolumetric ventricular relaxation and continues during rapid filling.[29] During early filling, suction causes pressure to fall despite the ventricle is filling. Therefore, reduced suction shifts the left corner of the pressure-volume loop toward a higher minimum diastolic pressure.

Diastolic suction is directly related to the apex-to-base DIVPD.[10–13] However, only 2 previous studies have measured DIVPDs in the human heart. Firstenberg et al[14] measured DIVPDs in the range of our study by using micromanometry. The same group has shown in patients with hypertrophic cardiomyopathy that DIVPDs are lower than in healthy subjects and improve after percutaneous septal ablation.[22] Although experimental studies have found that DIVPGs are depressed or even abolished after chronic pacing-induced heart failure,[17,18] ours is the first study to describe DIVPDs in a relatively wide population of patients with DCM.

Physiological Determinants of Diastolic Suction

At the cardiomyocyte level, diastolic suction involves deformation of the protein titin when sarcomeres are stretched above and shortened below slack length.[30] At the chamber level, the major determinant of diastolic suction is the elastic energy stored during systole. To generate elastic potential energy, LV volume must fall under a critical value during contraction. This minimal end-systolic volume required to generate suction equals the equilibrium volume, the latter designating the volume of the fully relaxed ventricle at zero pressure.[9] If either the equilibrium volume decreases or the

TABLE 3. Doppler-Derived Diastolic Hemodynamic Data

	Patients With Dilated Cardiomyopathy			Healthy Volunteers (n=20)	
	Full Group (n=40)	Stress Group (n=20)			
		Baseline	Dobutamine	Baseline	Dobutamine
Transmitral flow velocity data					
E-wave velocity, cm/s	77±31	79±31	83±36†	87±10	107±18*
A-wave velocity, cm/s	65±26†	68±29	79±31	50±10	64±15*
E/A velocity ratio	1.5±1.2	1.6±1.2	1.3±1.0	1.8±0.4	1.8±0.5
Time to E wave, ms	79±16†	78±15	68±26*	61±15	56±15
Deceleration time, ms	189±77†	190±72	217±70*	233±36	230±38*
Total filling time, ms	336±129†	287±91	270±96†	426±95	404±104
Isovolumic relaxation time, ms	97±24†	93±33	80±25*†	54±10	42±10
Flow propagation velocity, cm/s	31±12†	30±7	42±19†	64±13	96±28*
DIVPG pressure data					
Peak total DIVPD, mm Hg	1.2±0.6†	1.3±0.7	1.6±0.8†	2.5±0.8	3.6±1.1*
Peak inertial DIVPD, mm Hg	2.0±1.0†	2.0±1.1	2.4±1.3†	3.7±1.1	5.1±2.2*
Peak convective DIVPD, mm Hg	−1.8±1.2†	−1.9±1.2	−1.9±1.3†	−2.5±0.8	−4.0±1.4*
DIVPG temporal data					
DIVPD onset, ms	−16±13†	−12±14	−17±12	−29±11	−19±9
Time to peak DIVPD, ms	25±12†	28±15	21±10*†	16±9	14±12
Time to inertial DIVPD, ms	43±18†	46±21	38±19†	29±11	28±11
Time to convective DIVPD, ms	77±17†	73±18	68±25	61±16	57±16
Pressure gradient time delay, ms	124±43†	121±34	93±39*†	45±10	43±17

*$P<0.05$, dobutamine vs baseline for the same subject; †$P<0.05$, patients with dilated cardiomyopathy vs healthy volunteers for the same phase.

end-systolic volume rises, the ventricle becomes unable to generate suction.[9,17,18] For the present study, we used measurements of systolic function as clinically available indexes to account for this mechanism, and, in agreement with previous studies,[14,16] they correlated well with DIVPDs. Additional previously reported determinants of suction are the time constant of LV relaxation[29] and the degree of large-scale LV torsion and twist.[17]

Although the adverse effect of the convective deceleration forces has been reported in canine right ventricles,[19] deleterious convective deceleration had never been described in the LV. Because of its effects on the ventriculo:annular disproportion, LV dilatation "per se" impairs LV filling by this mechanism.

Effects of Stress on Diastolic Suction

The observation of a limited suction response to dobutamine in patients with DCM helps to explain why LV filling pressures may rise disproportionately during stress, leading to exercise-related dyspnea in these subjects. In the normal LV, β-adrenergic stimulation increases contractility, myocardial restoring forces and the resulting ventricular suction.[8,9,16] Another important effect of increased β-adrenergic tone is shortening filling time, an effect that could reduce the filling volume and elevate diastolic pressures. However, increased diastolic suction facilitates rapid filling and lowers minimum LV pressure.[13,31] Consequently, enhanced diastolic suction acts as a compensatory mechanism to maintain low pulmonary pressures in situations of increased contractility.

Hypothetically, this compensatory mechanism could be particularly helpful in patients with DCM, because they depend on an adequate end-diastolic volume to maintain cardiac output, and because they have chronically elevated filling pressures at rest. However, the present study shows that in contrast to controls, cardiomyopathic ventricles show abnormal suction at baseline and have a limited ability to recruit suction when undergoing inotropic stimulation. Total DIVPD increased by 23% in patients with DCM (albeit statistically nonsignificant, probably because of sample size), which was much lower than the 40% observed in volunteers. However, the effect of dobutamine on the time constant of relaxation is equivalent in patients with DCM and in healthy volunteers.[32] Consequently, we believe that although related, relaxation and diastolic suction provide complementary information on filling dynamics.

As opposed to what is seen in normal hearts, minimum diastolic pressure of failing ventricles rises during exercise.[31] It is very likely that the limited suction reserve recruitable by inotropic stimulation is a major determinant of this abnormal behavior induced by exercise. This issue deserves further clarification in future studies designed to specifically analyze DIVPGs during exercise.

Regional Homogeneity in the Development of DIVPGs

Diastolic suction and DIVPDs are sensitive to subtle changes of regional recoil induced by ischemia.[15,33] Thus, uncoordinated regional ventricular function is a major cause of

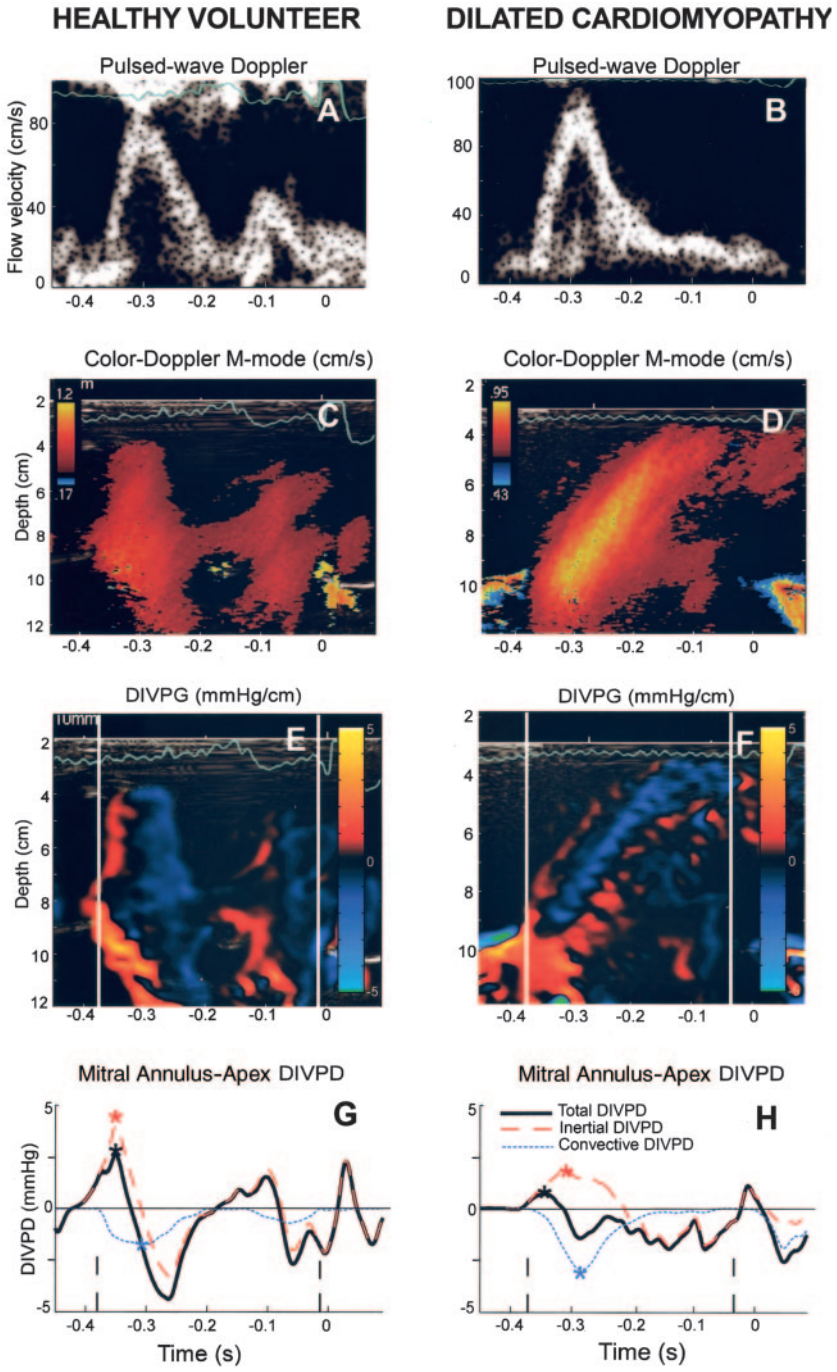

Figure 3. Doppler-derived analysis of diastolic filling in representative examples from a healthy volunteer (A, C, E, and G) and a patient with DCM (B, D, F, and H). A and B, Pulsed-wave Doppler flow velocity. C and D, Raw CDMM recordings. E and F, DIVPG maps. G and H, Charts showing total DIVPD curves and their components; peak values are marked with an asterisk. Vertical lines in panels E through H account for filling onset and end.

prolonged relaxation and abnormal diastolic suction. We believe that parametric images help to analyze this issue. With this visualization, it can bee seen that DIVPGs are developed nonsimultaneously along the LV longitudinal axis. In healthy volunteers, local temporal delay was very small, and DIVPGs reach their maximum almost simultaneously along the LV long axis. This was visualized as a very steep wave front in the DIVPG tracing and a high DIVPD. In contrast, in patients with DCM, the peak value of the DIVPG was reached at different moments along the long-axis cavity, and, by this mechanism, suction becomes disorganized, the time delay is prolonged, and the DIVPD is reduced.

Clinical Implications

These observations suggest a mechanism by which cardiac resynchronization therapy can hypothetically improve filling of DCM ventricles. If true, DIVPG analysis could be potentially helpful to predict the response or to optimize resynchronization therapy. Similarly, DIVPGs could provide further understanding on the mechanisms of infarct exclusion surgery. We believe these potential clinical applications deserve further investigation.

Pulsed-wave Doppler is the method most frequently used in clinical practice to assess the state of LV relaxation, compliance, and filling pressures. However, this method may

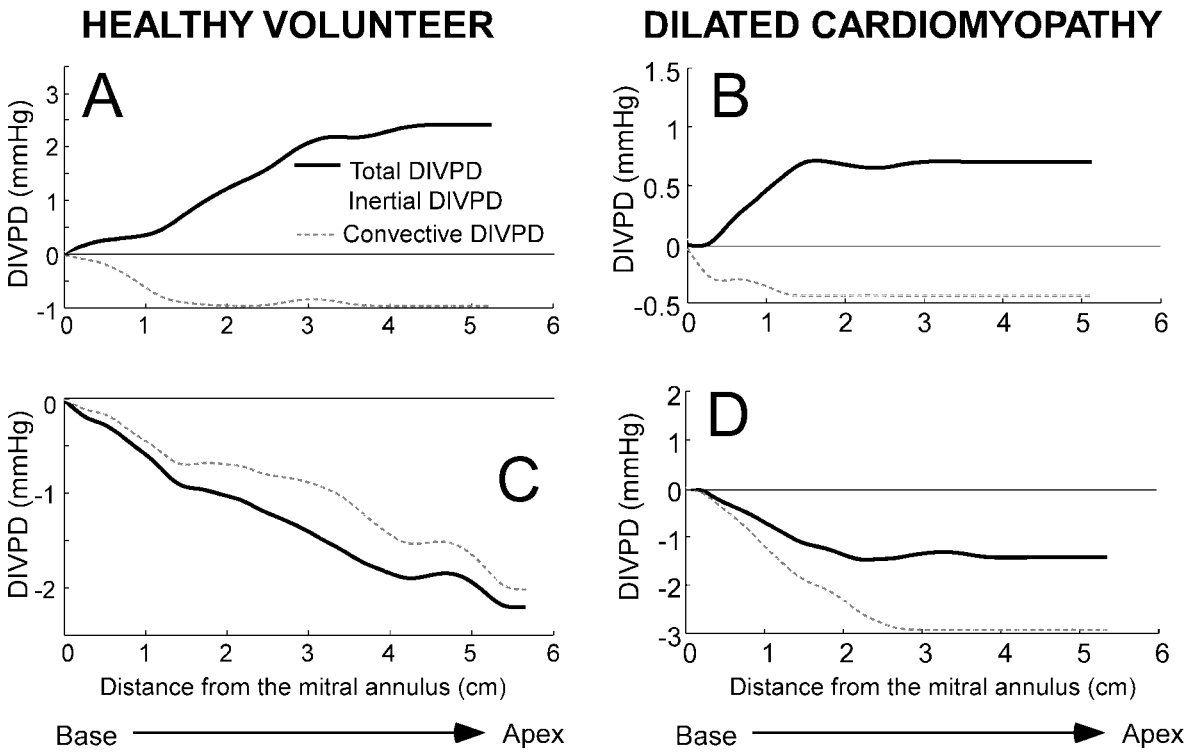

Figure 4. Spatial distribution of DIVPDs. Development of DIVPDs (vertical axis) along the LV long axis (horizontal axis) are illustrated for subjects shown in Figure 3, at the time of the peak total DIVPD (A and B) and at the time of peak transmitral flow velocity (C and D).

be limited to fully characterize diastolic physiology in a particular patient.[3] Our study suggests that complementary information on diastolic physiology can be obtained in the clinical setting by the analysis of DIVPGs.

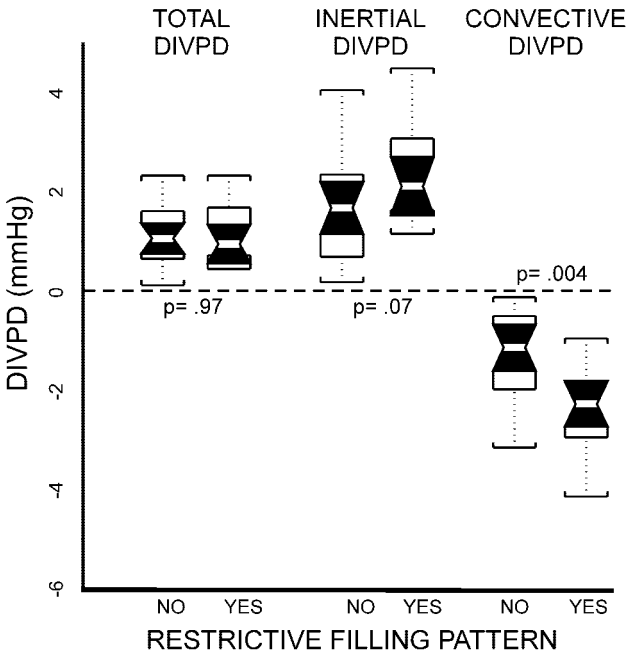

Figure 5. DIVPD analysis of patients with DCM according their transmitral filling pattern. Box plots represent 50th (white lines), 25th, and 75th percentile values as well as limits of the distribution (whiskers). Shaded zones account the 95% confidence interval for the median.

Study Limitations

A 1-dimensional trajectory is assumed in Euler's equation. Although filling flow follows a slightly curvilinear trajectory, good accuracy has been demonstrated for this method for measuring DIVPDs.[21,22] In severely dilated ventricles, however, the error related to the 1-dimensional simplification may be higher. In these situations, it is important to guide M-mode by 2-dimensional color Doppler, focusing on a coaxial interrogation of flow. Although we did not find this phenomenon in our study, in situations in which 2-dimensional Doppler shows a tightly curved trajectory, magnetic resonance is a feasible alternative for measuring DIVPDs.[34]

Also, the assumption of unidirectionality has not been specifically tested for isovolumic flows. However, our validation study suggests a reasonable accuracy of the method to measure DIVPD onset. During isovolumic relaxation, the LV untwists, rotates, and changes from spherical to an ellipsoidal shape.[13] A backward expansion wave is generated by these transformations that shifts the blood column toward the apex.[29] On the basis of these low-velocity flows, we were able to visualize DIVPGs during isovolumic relaxation (see Figure 2A).

Conclusions

Patients with DCM show an abnormally low diastolic suction as well as a blunted capacity to recruit suction with stress. Reduced diastolic suction is the consequence not only of a lower impulse due to depressed elastic recoil but also of relatively higher deleterious convective forces. By raising the ventriculo:annular disproportion, chamber remodeling proportionally increases convective deceleration and adversely affects LV filling. These previously unreported mechanisms

TABLE 4. Determinants of Inertial, Convective, and Total DIVPDs

	Inertial DIVPD			Convective DIVPD			Total DIVPD		
	β_{stand}	R_{part}	P	β_{stand}	R_{part}	P	β_{stand}	R_{part}	P
Variables in the model									
E-wave velocity	0.58	0.73	<0.0001	−1.38	−0.66	0.001			
Ejection fraction	0.54	0.70	<0.0001				0.61	0.46	0.0003
VA disproportion				−0.71	−0.27	0.04	−0.57	−0.32	0.01
E-wave velocity and EF interaction				1.05	0.34	0.009	0.58	0.43	0.0007
Adjusted R^2		0.69			0.77			0.59	

Multivariate linear regression models selected from a priori specified variables. β_{stand} indicates standardized linear regression coefficient; R_{part}, partial correlation coefficient; and VA, ventriculo:annular.

of diastolic dysfunction can now be studied noninvasively in the clinical setting.

Acknowledgments

This study was supported in part by grants PI03/1220, BF03/00031 (to R. Yotti), and G03/185 Nodo UNED (partial support to M. M. Desco) of the Instituto de Salud Carlos III, Spain, and by a grant of the Sociedad Española de Cardiología.

References

1. Vanoverschelde JL, Raphael DA, Robert AR, Cosyns JR. Left ventricular filling in dilated cardiomyopathy: relation to functional class and hemodynamics. *J Am Coll Cardiol*. 1990;15:1288–1295.
2. Xie GY, Berk MR, Smith MD, Gurley JC, DeMaria AN. Prognostic value of Doppler transmitral flow patterns in patients with congestive heart failure. *J Am Coll Cardiol*. 1994;24:132–139.
3. Garcia MJ. Diagnostico y guia terapeutica de la insuficiencia cardiaca diastolica. *Rev Esp Cardiol*. 2003;56:396–406.
4. Sabbah HN, Stein PD. Pressure-diameter relations during early diastole in dogs: incompatibility with the concept of passive left ventricular filling. *Circ Res*. 1981;48:357–365.
5. Yellin EL, Hori M, Yoran C, Sonnenblick EH, Gabbay S, Frater RW. Left ventricular relaxation in the filling and nonfilling intact canine heart. *Am J Physiol*. 1986;250:H620–H629.
6. Yellin EL, Meisner JS. Physiology of diastolic function and transmitral pressure-flow relations. *Cardiol Clin*. 2000;18:411–433.
7. Katz LN. The role played by the ventricular relaxation process in filling the left ventricle. *Am J Physiol*. 1930;95:542–553.
8. Bell SP, Fabian J, LeWinter MM. Effects of dobutamine on left ventricular restoring forces. *Am J Physiol*. 1998;275:H190–H194.
9. Nikolic S, Yellin EL, Tamura K, Vetter H, Tamura T, Meisner JS, Frater RW. Passive properties of canine left ventricle: diastolic stiffness and restoring forces. *Circ Res*. 1988;62:1210–1222.
10. Ling D, Rankin JS, Edwards CHD, McHale PA, Anderson RW. Regional diastolic mechanics of the left ventricle in the conscious dog. *Am J Physiol*. 1979;236:H323–H330.
11. Falsetti HL, Verani MS, Chen CJ, Cramer JA. Regional pressure differences in the left ventricle. *Cathet Cardiovasc Diagn*. 1980;6:123–134.
12. Courtois M, Kovacs SJ Jr, Ludbrook PA. Transmitral pressure-flow velocity relation: importance of regional pressure gradients in the left ventricle during diastole. *Circulation*. 1988;78:661–671.
13. Nikolic SD, Feneley MP, Pajaro OE, Rankin JS, Yellin EL. Origin of regional pressure gradients in the left ventricle during early diastole. *Am J Physiol*. 1995;268:H550–H557.
14. Firstenberg MS, Smedira NG, Greenberg NL, Prior DL, McCarthy PM, Garcia MJ, Thomas JD. Relationship between early diastolic intraventricular pressure gradients, an index of elastic recoil, and improvements in systolic and diastolic function. *Circulation*. 2001;104:I-330–I-335.
15. Bell SP, Fabian J, Watkins MW, LeWinter MM. Decrease in forces responsible for diastolic suction during acute coronary occlusion. *Circulation*. 1997;96:2348–2352.
16. Udelson JE, Bacharach SL, Cannon RO III, Bonow RO. Minimum left ventricular pressure during beta-adrenergic stimulation in human subjects: evidence for elastic recoil and diastolic "suction" in the normal heart. *Circulation*. 1990;82:1174–1182.
17. Bell SP, Nyland L, Tischler MD, McNabb M, Granzier H, LeWinter MM. Alterations in the determinants of diastolic suction during pacing tachycardia. *Circ Res*. 2000;87:235–240.
18. Solomon SB, Nikolic SD, Glantz SA, Yellin EL. Left ventricular diastolic function of remodeled myocardium in dogs with pacing-induced heart failure. *Am J Physiol*. 1998;274:H945–H954.
19. Pasipoularides A, Shu M, Shah A, Tucconi A, Glower DD. RV instantaneous intraventricular diastolic pressure and velocity distributions in normal and volume overload awake dog disease models. *Am J Physiol Heart Circ Physiol*. 2003;285:H1956–H1965.
20. Bermejo J, Antoranz JC, Yotti R, Moreno M, Garcia-Fernandez MA. Spatio-temporal mapping of intracardiac pressure gradients: a solution to Euler's equation from digital postprocessing of color Doppler M-mode echocardiograms. *Ultrasound Med Biol*. 2001;27:621–630.
21. Greenberg NL, Vandervoort PM, Firstenberg MS, Garcia MJ, Thomas JD. Estimation of diastolic intraventricular pressure gradients by Doppler M-mode echocardiography. *Am J Physiol*. 2001;280:H2507–H2515.
22. Rovner A, Smith R, Greenberg NL, Tuzcu EM, Smedira N, Lever HM, Thomas JD, Garcia MJ. Improvement in diastolic intraventricular pressure gradients in patients with HOCM after ethanol septal reduction. *Am J Physiol Heart Circ Physiol*. 2003;285:H2492–H2499.
23. Yotti R, Bermejo J, Antoranz JC, Rojo-Alvarez JL, Allue C, Silva J, Desco MM, Moreno M, Garcia-Fernandez MA. Noninvasive assessment of ejection intraventricular pressure gradients. *J Am Coll Cardiol*. 2004;43:1654–1662.
24. Yotti R, Bermejo J, Desco MM, Antoranz JC, Rojo-Alvarez JL, Cortina C, Allue C, Rodriguez-Abella H, Moreno M, Garcia Fernandez MA. Doppler-derived ejection intraventricular pressure gradients provide a reliable assessment of left ventricular systolic chamber function. *Circulation*. 2005;112:1771–1779.
25. Nijland F, Kamp O, Karreman AJ, van Eenige MJ, Visser CA. Prognostic implications of restrictive left ventricular filling in acute myocardial infarction: a serial Doppler echocardiographic study. *J Am Coll Cardiol*. 1997;30:1618–1624.
26. Appleton CP, Firstenberg MS, Garcia MJ, Thomas JD. The echo-Doppler evaluation of left ventricular diastolic function: a current perspective. *Cardiol Clin*. 2000;18:513–546.
27. Steine K, Flogstad T, Stugaard M, Smiseth OA. Early diastolic intraventricular filling pattern in acute myocardial infarction by color M-mode Doppler echocardiography. *J Am Soc Echocardiogr*. 1998;11:119–125.
28. Harrell FE. Hmisc and Design S-Plus function library. Available at: http://biostat.mc.vanderbilt.edu/twiki/bin/view/Main/RS. Accessed July, 2005.
29. Wang Z, Jalali F, Sun YH, Wang JJ, Parker KH, Tyberg JV. Assessment of left ventricular diastolic suction in dogs using wave-intensity analysis. *Am J Physiol Heart Circ Physiol*. 2005;288:H1641–H1651.
30. Kass DA, Bronzwaer JG, Paulus WJ. What mechanisms underlie diastolic dysfunction in heart failure? *Circ Res*. 2004;94:1533–1542.
31. Cheng CP, Noda T, Nozawa T, Little WC. Effect of heart failure on the mechanism of exercise-induced augmentation of mitral valve flow. *Circ Res*. 1993;72:795–806.
32. Parker JD, Landzberg JS, Bittl JA, Mirsky I, Colucci WS. Effects of beta-adrenergic stimulation with dobutamine on isovolumic relaxation in the normal and failing human left ventricle. *Circulation*. 1991;84:1040–1048.
33. Courtois M, Kovacs SJ, Ludbrook PA. Physiological early diastolic intraventricular pressure gradient is lost during acute myocardial ischemia. *Circulation*. 1990;81:1688–1696.
34. Thompson RB, McVeigh ER. Fast measurement of intracardiac pressure differences with 2D breath-hold phase-contrast MRI. *Magn Reson Med*. 2003;49:1056–1066.